

Searching for p -modes in η Boötis & Procyon using MOST satellite data

D. B. Guenther¹, T. Kallinger², P. Reegen², W. W. Weiss², J. M. Matthews³,
R. Kuschnig³, A. F. J. Moffat⁴, S. M. Rucinski⁵, D. Sasselov⁶ and
G. A. H. Walker³

¹Institute for Computational Astrophysics, Department of Astronomy and Physics,
Saint Marys University, Halifax, NS B3H 3C3, Canada

² Institut für Astronomie, Türkenschanzstrasse 17, 1180 Vienna, Austria

³ Department of Physics and Astronomy, University of British Columbia, 6224
Agricultural Road, Vancouver, BC B6T 1Z1, Canada

⁴ Département de Physique, Université de Montréal C. P. 6128, Succursale :
Centre-Ville, Montréal, QC H3C 3J7 and
Observatoire Astronomique du Mont Mégantic, Canada

⁵ Department of Astronomy and Astrophysics, David Dunlap Observatory,
University of Toronto, P. O. Box 360, Richmond Hill, ON L4C 4Y6, Canada

⁶ Harvard-Smithsonian Center for Astrophysics, 60 Garden Street,
Cambridge, MA 02138

Abstract

We present frequency analyses of new photometry obtained in 2005 by the MOST¹ (*Microvariability & Oscillations of STars*) satellite of two solar-type stars, η Boötis and Procyon, and reanalyses of MOST data of these stars obtained in 2004. With improved strategies to identify and correct stray light artifacts in the MOST Fabry Imaging data, we produce amplitude spectra from the reduced data and compare them to p -mode oscillation spectra computed from stellar models. We confirm the null result from the 2004 MOST observations of Procyon. We find no evidence for spectral power with regular spaced frequencies characteristic of radial p -modes, nor do we find excess power in the expected p -mode frequency range. Consequently, we argue the absence of p -mode oscillations in Procyon exceeding our detection limit of about 10ppm.

¹Based on data from the MOST satellite, a Canadian Space Agency mission, jointly operated by Dynacon Inc., the University of Toronto Institute for Aerospace Studies and the University of British Columbia, with the assistance of the University of Vienna.

For η Boo, the frequencies present in the 2005 data do not match within the resolution those identified in the 2004 data after excluding all frequencies we suspect to be due to stray light contamination. However, there is clear evidence for excess power within the p -mode range predicted by models. We discuss the implications of these results for mode lifetimes in these stars and the sensitivity of high-precision photometry to solar-type oscillations in the presence of granulation.

Introduction

Eigenfrequency spectra of acoustic oscillations have been observed in solar-type stars through groundbased spectroscopic measurements of radial velocity, especially with the advent of the few-m/s precision developed for extrasolar planet searches. The study of such p -modes photometrically requires a precision of a few parts per million (ppm) or less, which can only be achieved reliably from space. The MOST space mission, lead by J. Matthews and first reviewed by Walker et al. 2003, was designed to obtain such precision for a few bright stars. The long, nearly continuous time coverage possible with MOST would also make it possible to resolve fine structure in the p -mode eigenspectrum for asteroseismic modeling.

Two early MOST targets were Procyon (Matthews et al. 2004) and η Boötis (Guenther et al. 2005), both observed in 2004 for about a month each. In the former, no p -modes were detected, with strong upper limits on amplitude and mode lifetime. In the latter, radial p -modes were identified that are consistent with a stellar structure model appropriate to η Boo, and which extend to low overtones the sequence of modes identified by Kjeldsen et al. (2003) in their spectroscopic data. The astrophysical implications of the results warranted second sets of photometry to confirm, refine or deny the original findings. For this reason, both stars were chosen to be reobserved by MOST in 2005.

The trail of two stars

Procyon and η Boo are more massive than the Sun and are in their post-main-sequence phase of evolution. They have convective envelopes but with different depths. This makes these stars attractive targets to help quantify the driving of p -modes by turbulent convection, the mechanism believed to operate in solar-type stars, as in the Sun.

The coupling between the pressure variations associated with p -modes and their driving source, the convective motions, is greatest in the very outermost layers of the convective envelope, in a thin region called the superadiabatic layer. Numerical hydrodynamical simulations of stellar convection (Robinson

et al. 2005) show that the convective velocities are greater in stars with thinner convection zones (such as found in the post main-sequence stars Procyon and η Boo) than those with deeper convective envelopes like the Sun. If the amplitudes of the p -mode pulsations correlate with the maximum turbulent velocities, and hence the depth of the convection zone, then the amplitudes of the p -modes in stars like Procyon and η Boo should be greater than those observed in the Sun (Christensen-Dalsgaard & Frandsen 1993; Kjeldsen & Bedding 1995; Houdek et al. 1999).

Attempts to observe p -modes on these stars from the ground have yielded mixed results. For Procyon, the groundbased radial velocity observations show an enhanced region of power in the frequency range 0.5 – 1.5 mHz (e.g., Brown et al 1991; Martic et al. 1999; Eggenberger et al. 2004). The identification of individual peaks and regular spacings is less certain, although both Martic et al. (1999) and Eggenberger et al. (2004) find a frequency spacing of 55 μ Hz, which is consistent with model predictions (Chaboyer et al. 1999). In the case of η Boo, several groundbased campaigns have yielded plausible individual p -mode identifications (Kjeldsen et al. 2003, Carrier et al. 2005). They find a spacing of 40 μ Hz, consistent with models. However, there is little coincidence of the actual identified frequencies between the two groups, and even between observing runs by the same group from epoch to epoch.

The results on Procyon and η Boo from MOST's first year of operation have already been published (Matthews et al. 2004; Guenther et al. 2005). We reported a null detection for Procyon and a possible detection of radial p -modes on η Boo. The Procyon null detection was a surprise since we expected the amplitudes of the oscillations, as consequence of its very thin convective envelope, to be large enough to be detectable above the noise level of a few ppm in the MOST photometry. The tentative detection of p -modes on η Boo was also not quite what we expected. We had expected to see a clear and unambiguous signature of p -modes. What we saw though were many peaks in the spectrum, of which less than a third could be associated with the radial p -modes of our models. Other peaks in the spectrum of comparable amplitudes could not be unambiguously identified because stellar models appropriate to η Boo show a rich and complex eigenspectrum of nonradial modes which are very sensitive to changes in metallicity, convection parameters and envelope models. This ambiguity makes exact nonradial mode identification in our MOST photometry virtually impossible without additional information on stellar fundamental parameters derived with techniques other than asteroseismology.

In this paper we present the new sets of MOST photometry of Procyon and η Boo obtained in 2005, and a revised strategy to identify p -mode signals in the data. Much of this strategy involves identifying and removing artifacts in the MOST data introduced by stray light from scattered Earthshine. We apply this

to the new data and the previously published 2004 photometry, and compare the resulting frequency spectra for each star to stellar models. We also discuss the possibility of short p -mode lifetimes and show the consequences of short lifetimes on the observations.

Observations & Data Analysis

The MOST microsatellite houses a 15-cm telescope which feeds a CCD photometer through a custom broadband optical filter. For the brightest stellar targets and the highest photometric precision, starlight is directed through a Fabry microlens to produce a fixed image of the telescope pupil covering about 1500 pixels on the detector. MOST is in a near-polar Sun-synchronous orbit of altitude 820 km, from which it can monitor stars continuously for up to two months within a 54° -wide viewing zone. The instrument is capable of achieving noise levels in the Fourier domain for very bright stars of about 1 ppm at frequencies above about 1 – 2 mHz.

It was recognized in the earliest observations (e.g., Matthews et al. 2004; Rucinski et al. 2004) that stray light entering the Fabry field due to scattered Earthshine was modulated with the MOST orbital period. This introduces artifacts in the data at the satellite orbital frequency and its harmonics, and other modulation terms. These effects, other aspects of spacebased CCD photometry, and how they are dealt with in MOST Fabry Imaging photometric reductions, are described in more detail by Reegen et al. (2006) and revisited here in Section *Stray light processing*.

MOST photometry of Procyon and η Boo

The data set for Procyon consists of two runs: 32 days in January 2004 (Matthews et al. 2004), and 17 days in January 2005 (this paper). For η Boo, the runs cover: 27 days during April–May 2004 (Guenther et al. 2005) and 21 days during March–April 2005. In Table 1 we summarize the properties of all four observing runs, listing the start and end dates of each run, its duration, exposure time, number of exposures, duty cycle, and resulting frequency resolution.

Stray light processing

The photometric signal from a MOST Fabry Imaging target star arrives on the CCD in an annulus (see Fig. 1 in Reegen et al. 2006). We define the “Fabry image” to be the image of the telescope entrance pupil produced by a Fabry lens close to the CCD, the “target pixels” to be those pixels located within the

Table 1: Basic parameters of the MOST photometry.

Target	Procyon		η Boo	
Year	2004	2005	2004	2005
Date	03 Jan 09 Feb	24 Jan 10 Feb	13 Apr 11 May	31 Mar 21 Apr
Duration [d]	30.98	16.98	26.96	20.59
Exposure [s]	0.9	1	6	7
# of Exposures	86446	48840	87806	55101
Duty cycle [%]	96.9	99.8	75.4	92.9
Resolution [μ Hz]	0.37	0.68	0.43	0.56

annulus, and the “background pixels” to be the remaining pixels in the square CCD subraster which represents the Fabry field stored and downloaded from the satellite. The pixels (58×58 in 2004 and 60×60 in 2005) in the Fabry field are binned 2×2 before photometric processing. The numbers of binned target pixels and binned background pixels are about equal: ~ 450 each. The Fabry micro-optics were designed to guide all light from a target star entering the telescope aperture (even with changing incident angles due to spacecraft pointing errors) to the same set of pixels on the CCD. The stellar signal in the target pixels is nearly independent of the small level of satellite pointing jitter.

Photometry obtained from MOST includes a periodic, amplitude-modulated signal due to stray light entering the instrument from scattered Earthshine. The stray light variation has a non-sinusoidal shape and its amplitude and shape depend on the observing season, the location of the star relative to the illuminated limb of the Earth, and the orientation (roll) of the spacecraft. The relative effect of the stray light depends also on the brightness of the star. The most obvious effect of the stray light variation in frequency analysis of MOST data is a set of peaks in the Fourier domain at the MOST orbital frequency and its harmonics. Matthews et al. (2004) aggressively removed the power at those frequencies by treating the 2004 Procyon data with a running mean filter tuned to the orbital frequency of about $165 \mu\text{Hz}$. Guenther et al. (2005) applied a different reduction scheme, described in detail in Reegen et al. (2006), which looks for the correlation between the stray light signal in the target pixels and the stray light signal in the background pixels.

Because stray light does not uniformly illuminate the CCD, it is difficult to eliminate all of its contributions to the stellar time series, even with pixel decorrelation, and the remaining signal can be as large as 100 ppm in some cases. Most of our post-processing of the data is focused on removing this component and to estimate the level of contributions of non-stellar signal at a given

10 Searching for p -modes in η Boötis and Procyon using MOST satellite data

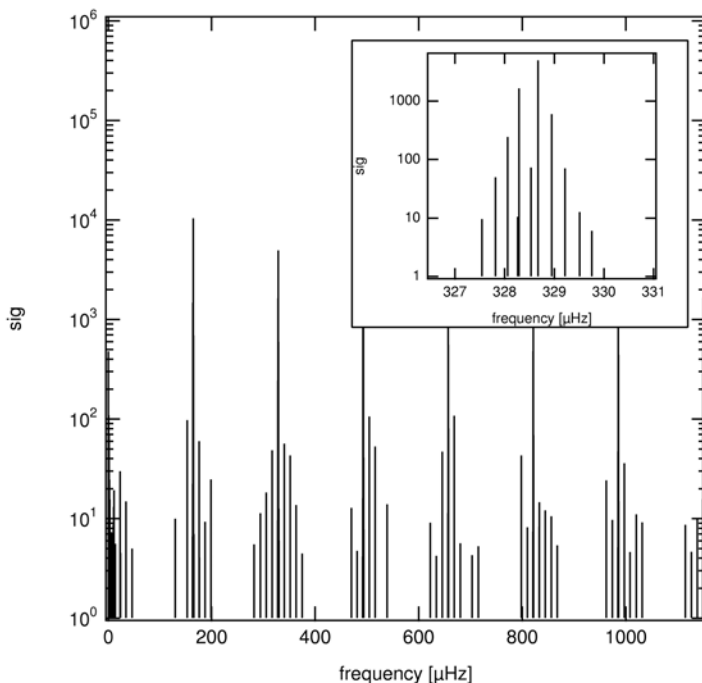


Figure 1: The spectral significance spectrum for the background time series (BTS) of Procyon 2004 data. The highest peaks are due to stray light correlated with orbital harmonics. The secondary peaks in the main figure are 1 cycle day⁻¹ aliases due to the changing albedo of the earth reflected sunlight. The insert shows a highly magnified portion of the graph surrounding one of the orbital peaks. The peaks shown in the insert, which lie very close to the orbital harmonic peak, are amplitude modulation peaks due to long period changes in the attitude of the MOST satellite.

frequency. We begin by removing white noise from both the background time series (BTS) and the target time series (TTS) by applying a Fourier transform algorithm to the data. The *SigSpec* routine (Reegen 2006, 2007) performs a Fourier transform on the time series data, picks out the peak which is statistically most likely to be real and not an artifact of noise (based on its amplitude and phase), assigns a probability to that peak, and then fits and removes the harmonic signal from the time series. The process is repeated until the peaks found are below a user-specified probability threshold. For well-sampled time series like the MOST photometry presented here, *SigSpec* and other Discrete Fourier Transforms give identical results. By assigning a probability to a given

frequency (and corresponding amplitude and phase) that it is not caused by white noise, *SigSpec* allows a more rigorous statistical treatment of the resulting amplitude spectrum. Specifically, a peak with a spectral significance equal to *sig* means that that signal would only occur once in 10^{sig} random Gaussian noise spectra. For example, a spectral significance of 6, means that that peak's amplitude, frequency and phase would only appear in one in a million Gaussian noise spectra. We have shown mathematically and through simulations that a spectral significance level ("sig", returned by *SigSpec*) of 5.6 corresponds roughly to a signal-to-noise ratio in amplitude of 4 for a non-modulated periodic wave (Reegen 2005, 2006).

Peaks with high spectral significance are very unlikely to be caused by white noise. Not all noise is white, nor is it necessarily all due to instrumental effects. For example, stars like Procyon and η Boo have surface convection zones, which produce granulation noise in the photometry whose amplitude will increase with decreasing frequency.

After applying *SigSpec* to the BTS in a threshold limited spectral significance spectrum we obtain, as presented in Section 3, only instrumental signal, as expected for the background. The same analysis applied to the TTS yields stellar plus instrumental signal, provided that the threshold limit is set high enough to reject random white noise. With the instrumental signal clearly identified in the BTS, our next step is to remove this signal from the TTS, leaving behind, presumably, the intrinsic stellar signal. In an early version of our reduction routine, we accomplished this by removing the corresponding significant peaks found in the BTS from the TTS. Of course, if there is any intrinsic stellar power coincidentally at those frequencies, it is also removed. A shortcoming of this approach is that – formally – a tiny signal in the BTS can eliminate a large signal in the TTS, which may actually be dominated by the stellar variations. To address this possibility, we transformed a given measured BTS signal amplitude to the (usually higher) intensity level of the TTS and assumed that stray light components are additive in the TTS.

Recognizing Artifacts in the data

Background signal

The background intensity consists mainly of three components: the bias level of the CCD, the stray light signal, and (as a minor component) the sky background. The stray light signal increases linearly with the exposure time while the bias level remains approximately constant.

After applying our analysis to the BTS of the 2004 Procyon observations, we obtain the spectral significance spectrum shown in Figure 1 (for spectral

12 Searching for p -modes in η Boötis and Procyon using MOST satellite data

significances ≥ 4). The largest significant peaks correspond to the expected orbital harmonics. The smaller peaks surrounding the largest peaks are side lobes separated by multiples of 1 cycle day^{-1} . The amplitude of the stray light is modulated by both the orbital period of the satellite and its Sun-synchronous nature, which brings MOST over a similar part of the Earth after one day, so similar albedo features affect the stray light as they rotate into view. There is additional structure (see inset in Figure 1) associated with the slower modulation of the stray light signal during the long observing run, as the orientation of the satellite orbit and the position of the star with respect to the illuminated Earth change. All of the peaks in the background spectrum, except those at very low frequencies near $0 \mu\text{Hz}$, are associated with stray light. The largest peaks at the orbital frequency and its first harmonic have amplitudes of 13.9 mmag and 6.4 mmag , respectively.

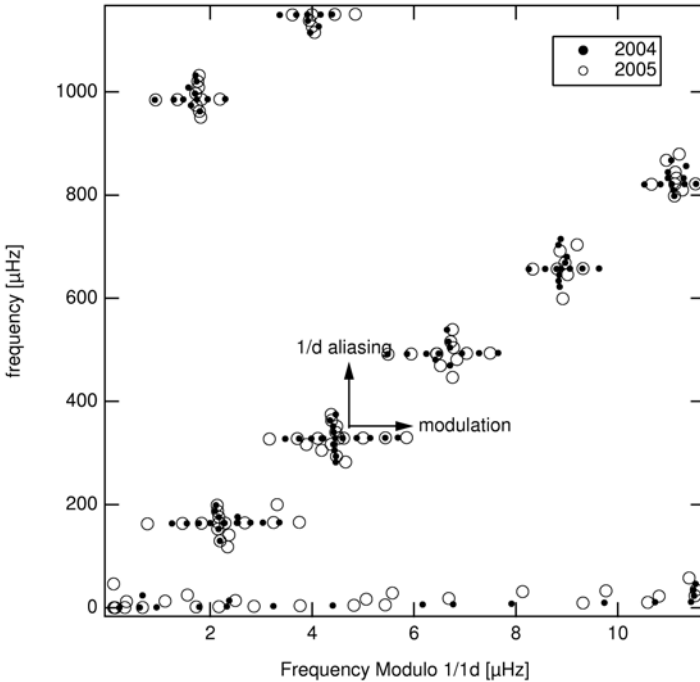


Figure 2: An echelle diagram with folding frequency $1/d^{-1}$ for the BTS of Procyon 2004 data, filled circles, and Procyon 2005 data, open circles. The distribution of peaks into "plus shaped crosses is due to both 1 cycle day^{-1} aliases and modulation effects on the orbital harmonics of stray light. The slope comes from the incommensurability of orbit and 1-day period.

The easiest way to distinguish the 1 d^{-1} side lobes from the amplitude modulation peaks is to fold the spectrum into an echelle diagram with a folding frequency of 1 cycle day^{-1} . In Figure 2, the frequencies of the peaks in the background spectral significance spectrum for the Procyon 2004 and 2005 data are plotted in this way (as dots and open circles, respectively). We are not concerned with the very low frequency peaks running along the bottom of Fig. 2, since the window function of the high-duty-cycle MOST data has little spectral leakage and this power does not contaminate the higher frequencies of interest for stellar p -modes. The remaining peaks fall nicely into groups, with the groups themselves falling along a diagonal line. The peaks within each group fall on a “+”-shaped orthogonal grid. Each group of peaks corresponds to an orbital harmonic. The vertically aligned peaks of each cross correspond to peaks that are 1 d^{-1} side lobes of the orbital harmonic. That is they correspond to $j \cdot f_o \pm k$ (1 cycle day^{-1}), where j is an integer corresponding to the order of the orbital harmonic, k is an integer corresponding to the order of the 1 day side lobe, and f_o is the orbital harmonic frequency (in units of cycles day^{-1}). The slow variation of the stray light signal over the duration of the run introduces beat frequencies in the Fourier Transform, which can be seen as the horizontally aligned peaks in each cross in Fig. 2. All the orbital and 1 d^{-1} side lobe peaks are amplitude-modulated but, in the case of the 2004 Procyon photometry, only the orbital harmonics themselves have large enough amplitudes to reveal modulation effects. In the case of η Boo, the amplitude modulation peaks are visible even for the higher-order 1 d^{-1} side lobes, i.e., $k \neq 1$.

Note that there are no other peaks in the spectral significance spectrum of the background. Our analysis has not only identified the periodic components in the background (in this case due to stray light), but suppressed any other peaks due to random white noise. In Figure 2, the orbital harmonics and 1 d^{-1} side lobes for the 2004 and 2005 Procyon data coincide. The peaks due to slower amplitude modulation do not match up, as expected, since the orientation of the MOST telescope was not exactly the same in both runs and the 2005 observations extended later into the season than those in 2004 (see Table 1). We can measure the variation in amplitude of an orbital harmonic as a function of time by splitting the BTS into subsets, as shown in Figure 3 for the three lowest orbital harmonics in both Procyon data sets, with running bins 4 days long spaced by 1-day intervals. The long-term amplitude modulation is comparable for all the 1-d^{-1} side lobe peaks around the orbital harmonic peaks.

The background spectra for the η Boo observing runs are more densely filled with stray-light-related signals. Both the orbital harmonics and the 1-d^{-1} side lobes of the orbital harmonics are modulated in amplitude. The increased number of peaks compared to those for Procyon is mainly due to the increased relative contribution of the stray light background since η Boo is more than 2

14 Searching for p -modes in η Boötis and Procyon using MOST satellite data

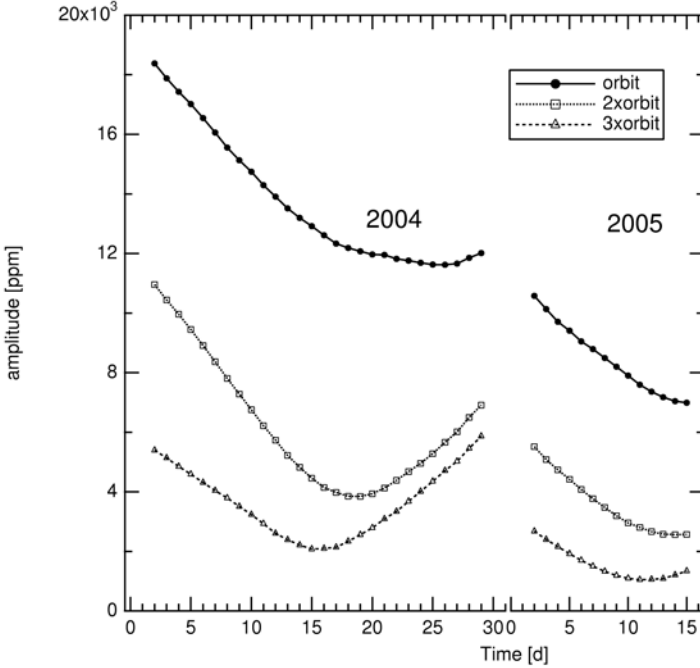


Figure 3: Modulation of the stray light amplitudes over the duration of the observations for Procyon 2004 and 2005 BTS data. The amplitude of the orbit and $1/d$ side lobe peaks in stray light change during the observing run due to changes in the attitude of the MOST satellite as it, and the earth, orbit the Sun.

magnitudes fainter than Procyon.

Target signal

Having identified the periodic stray light signals in the background pixels of the Fabry image, we then proceed to filter those signals from the target pixels.

As before, we first produce a spectral significance spectrum, now for the target time series (TTS). Because the stray light signal is periodic (albeit modulated), it is not identified as statistical noise and is not filtered by this process. The target spectral significance spectrum, therefore, contains both stray light signal and any other periodic variations intrinsic to the star. We have seen in Figure 2 that the orbital harmonics are accompanied by side lobes separated by $1 d^{-1}$. The long-term amplitude modulation is comparable for all the $1-d^{-1}$ side

lobes around each orbital harmonic. Therefore, most of the beat frequencies produced by that modulation have at least one companion 1 d^{-1} away, within a conservative frequency resolution given by $\pm 1/(\text{time span of the data})$. We assume that each peak in the target spectral significance spectrum which is part of a 1-d^{-1} pair is due to remaining stray light signal and we reject both. We stress that these pairs are not due to daily aliases produced by the spectral window function, as is a problem for ground-based observations, since MOST observations do not have daily gaps.

Not all stray light components are parts of 1-d^{-1} pairs. To filter out the remaining stray light signal, we search through the residual target spectral significance spectrum, identify and remove all peaks from the spectrum that match peaks in the background spectral significance spectrum. We consider peaks to match if their frequencies agree within the frequency resolution (see Table 1). This approach, unfortunately, may also remove any intrinsic stellar signal near those frequencies. To avoid removing a high amplitude target peak just because it is located close to the frequency of a very low amplitude background peak, we compare the amplitudes and re-introduce the removed frequency if the removed frequency's amplitude is much greater than the background peak's amplitude.

The approximate percentages of significant peaks we identify as instrumental and remove are: Procyon 2004, 70.3%; Procyon 2005, 74.4%, η Boo 2004 85%, and η Boo 2005, 84.6%. The approximate percentages of the frequency ranges covered by these instrumental signals (taking into account the inherent frequency resolutions of the data sets) are: Procyon 2004, 5.3%; Procyon 2005, 9.3%; η Boo 2004, 49.8% and η Boo 2005, 42.1%. If p -modes are present in our target spectral significance spectra, then these latter percentages represent approximately the percentage of p -mode peaks which have likely been filtered out along with the stray light signal.

Searching for p -modes

No p -modes in Procyon

In Figure 4, we plot an echelle diagram for the peaks in the filtered 2004 and 2005 Procyon data together. The echelle folding frequency is $53 \mu\text{Hz}$ (close to the average spacing predicted by stellar models) and the figure contains only frequencies which we are convinced are not contaminated by instrumental effects. No frequencies of the 2004 and 2005 data set overlap nor are there any obvious p -mode alignments in either data set. Note that because the 2005 run is shorter than the 2004 run, the noise level in the 2005 data is higher; hence, there are fewer peaks with $\text{sig} \geq 5.6$. The model frequencies also shown in this figure will be discussed later in this Section.

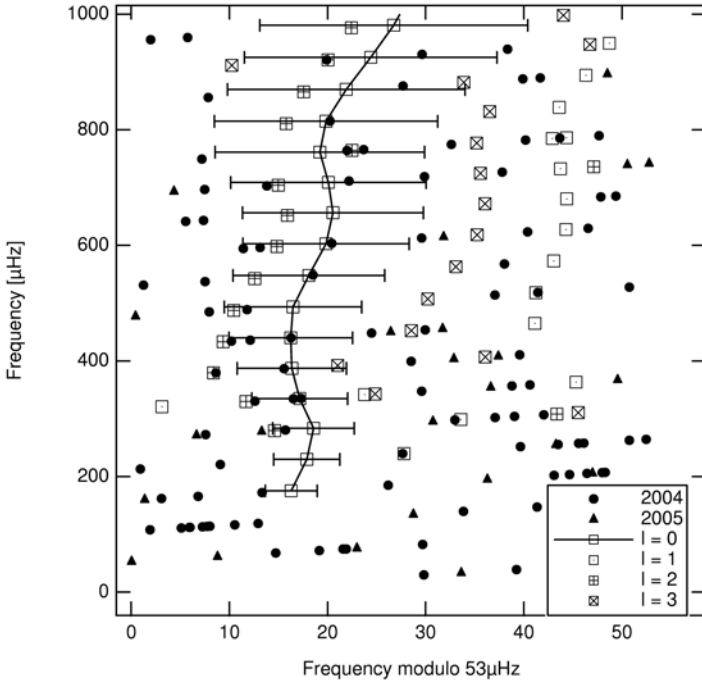


Figure 4: An echelle diagram comparing the Procyon 2004, filled circles, and Procyon 2005, filled triangles, spectral significance spectra to p -modes of models of Procyon (open symbols). The model mode frequencies are the average of all models that lie within 1σ of Procyon's mass, luminosity, and effective temperature (see Table 2). The error bars show the range of frequencies for each mode for models that lie within 1σ of Procyon's mass, luminosity, and effective temperature.

Ignoring the stray light and considering only true statistical noise for the 2004 Procyon data, the lowest peaks we can identify above the noise threshold (set at $\text{sig} = 4$) have amplitudes of about 10 ppm. The peaks from the 2004 spectrum with $\text{sig} \geq 5.6$ have amplitudes ≥ 12 ppm. For the 2005 Procyon data (shown in Fig. 5), the corresponding amplitudes are about 11 ppm and 14 ppm. The echelle structure of p -modes in Procyon may not exhibit as simple an asymptotic pattern as expected. To explore this, we have examined stellar models taken from one of the author's (DBGs) dense and extensive grids (Guenther et al. 2005). Using typical values for the temperature, luminosity and composition of Procyon, along with a mass constraint based on its binary orbit (Girard et al. 2000), we selected models in the grid that fall within 1σ

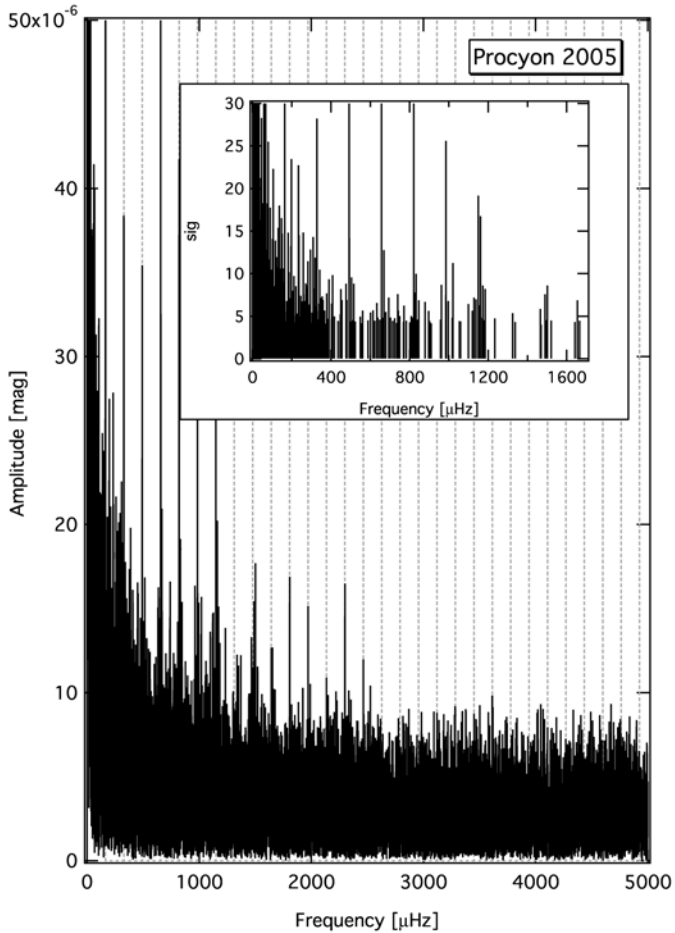


Figure 5: Amplitude spectrum of Procyon from stray light reduced MOST 2005 data. The vertical dashed lines correspond to the satellites orbit frequency (164.34 μHz) and its overtones. The corresponding spectral significance spectrum peaks for spectral significances greater than 4.0 are shown in the insert.

of these constraints. Because the models are based on standard physics, discrepancies between the observed oscillation spectrum and the model predicted spectra will highlight inadequacies in the models. For example, increasingly poorer fits at higher frequencies could indicate problems with modeling the sur-

face layers, such as those implied by the 0.25% discrepancy that exists between the Sun's observed frequencies and those of the standard solar model (Guenther & Brown, 2004). The adopted stellar parameters are listed in Table 2, and the average values (and standard deviations) of key properties of the best models are given in Table 3. Those properties are: mass, age, log effective temperature ($\log \text{Teff}$), log luminosity ($\log L/L_{\odot}$), mass of the convective envelope (M_{CE}), mass of the convective core (M_{CC}), acoustic cut-off frequency (ν_{cutoff}), characteristic p -mode frequency spacing ($\Delta\nu$), characteristic g -mode period spacing ($\Delta\Pi$), average large $l = 0$ frequency separation ($\langle \Delta\nu_0 \rangle$), average large $l = 1$ frequency separation ($\langle \Delta\nu_1 \rangle$), and average small $l = 0$ frequency separation ($\langle \delta\nu_0 \rangle$). The spacings are averaged over radial orders $n = 10\text{--}30$. For each set of constraints, properties are listed for the closest model and the average of all the models that lie within 1σ of the constraints. The uncertainties are standard deviations of the averages. The LT and LTM labels identify the constraints used on the models, with LT corresponding to luminosity and effective temperature and LTM corresponding to luminosity, effective temperature, and mass. The constraints are the uncertainties in Table 2.

Models constrained by the luminosity, surface temperature, and mass of Procyon have a characteristic spacing $\Delta\nu$ that varies as a function of $\log L/L_{\odot}$ and $\log \text{Teff}$ near Procyon's position in the H-R Diagram, as shown in the contour plot in Figure 6. Within the 1σ uncertainties for $\log L/L_{\odot}$ and $\log \text{Teff}$ (the boundaries of Fig. 6), $\Delta\nu$ varies from $53 \mu\text{Hz}$ to $56 \mu\text{Hz}$. Figure 4 is an echelle diagram with folding frequency $53 \mu\text{Hz}$ for the averaged values of the model $l = 0, 1, 2,$ and 3 p -mode frequencies for Procyon, compared to the identified 2004 and 2005 Procyon peaks with spectral significance ≥ 5.6 . The model frequencies shown are not taken from a single best-fitting model but are, for each mode, the numerical average of all the models with $Z=0.02$ that lie within 1σ of Procyon's mass, luminosity, and effective temperature constraints. The range of frequencies for the radial ($l = 0$) p -modes in all these accepted models is indicated by error bars in Figure 4. The p -mode frequency uncertainty due to mass, luminosity, and effective temperature constraints on the model increases with increasing frequency. Note that the p -mode frequencies for a given value of l are not scattered randomly between the error bars but align themselves along a vertical sequence which itself lies between the left and right edges defined by the uncertainty bars.

There is still no evidence in the MOST photometry to indicate p -modes in Procyon, not even an excess of power centred near $800 \mu\text{Hz}$. Either the p -mode luminosity amplitudes fall near or below the sensitivity of MOST after stray light filtering or the mode lifetimes are short enough to prevent clear identification in the complete data sets.

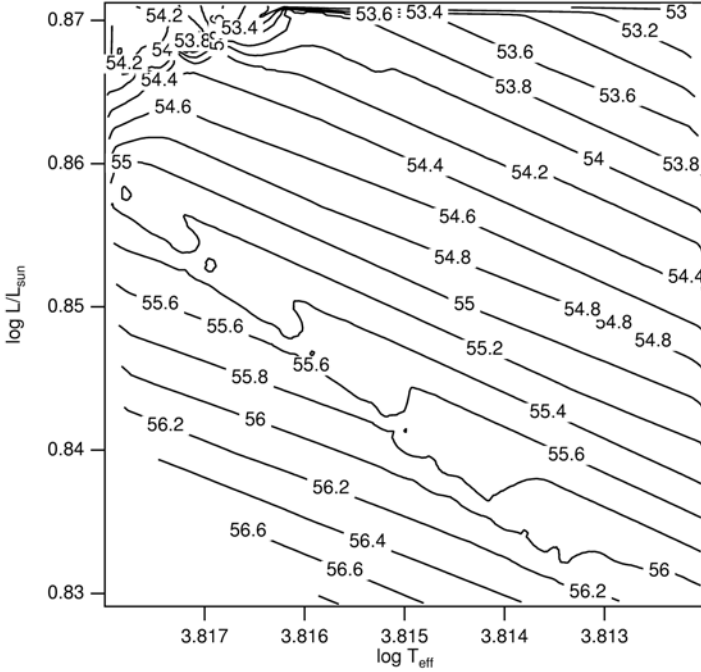


Figure 6: A contour plot showing the characteristic spacing $\Delta\nu$ for models of Procyon in the vicinity of its position in the HR-diagram. The log Teff and log L/L_{\odot} axis ranges correspond to the 1σ box around Procyons HR-diagram location. The contour labels are in units of μHz .

Possible p -modes in η Boo

We carried out identical filtering of the data for this star to remove first the d^{-1} multiplets, then the remaining background peaks. The more aggressive stray light filtering performed for the present study has eliminated all the peaks identified in 2004 as radial modes. Although these frequencies may still contain a significant amount of stellar signal, we are unable to confirm this. The echelle diagram of the identified intrinsic peaks in the MOST η Boo photometry is plotted in Figure 7.

For the 2004 η Boo data, the lowest peaks we can identify above the noise threshold set at $\text{sig} = 4$ have amplitudes of about 7 ppm. The 2004 peaks used for Fig. 7 with $\text{sig} \geq 5.6$ have amplitudes ≥ 9 ppm. For the 2005 data (see Fig. 8), the lowest peaks above the noise threshold ($\text{sig} = 4$) have amplitudes

Table 2: Properties of the MOST targets.

Name	Z	T_{eff}	L/L_{\odot}	M/M_{\odot}
Procyon	0.02	$6530 \pm 50\text{K}$	7.23 ± 0.35	1.497 ± 0.037
η Boo	0.04	$6028 \pm 45\text{K}$	9.02 ± 0.22	-

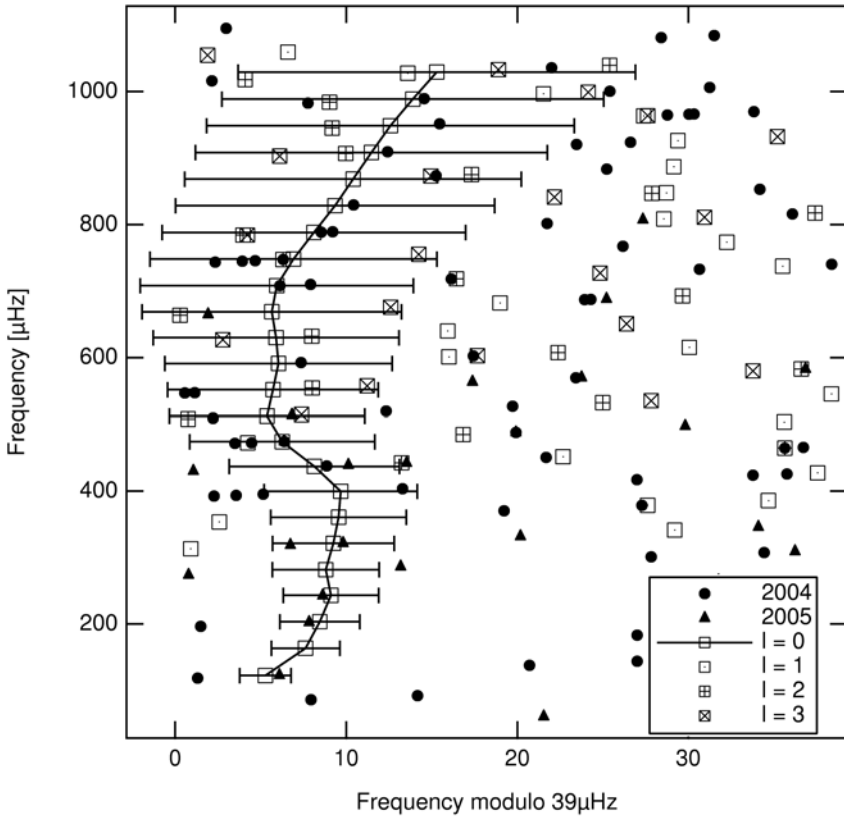


Figure 7: An echelle diagram comparing the η Boo 2004, filled circles, and η Boo 2005, filled triangles, spectral significance spectra to p -modes of models of η Boo (open symbols). The model mode frequencies are the average of all models that lie within 1σ of η Boos luminosity and effective temperature (Table 2). The error bars show the range of frequencies for each mode for models that lie within 1σ of η Boos luminosity, and effective temperature.

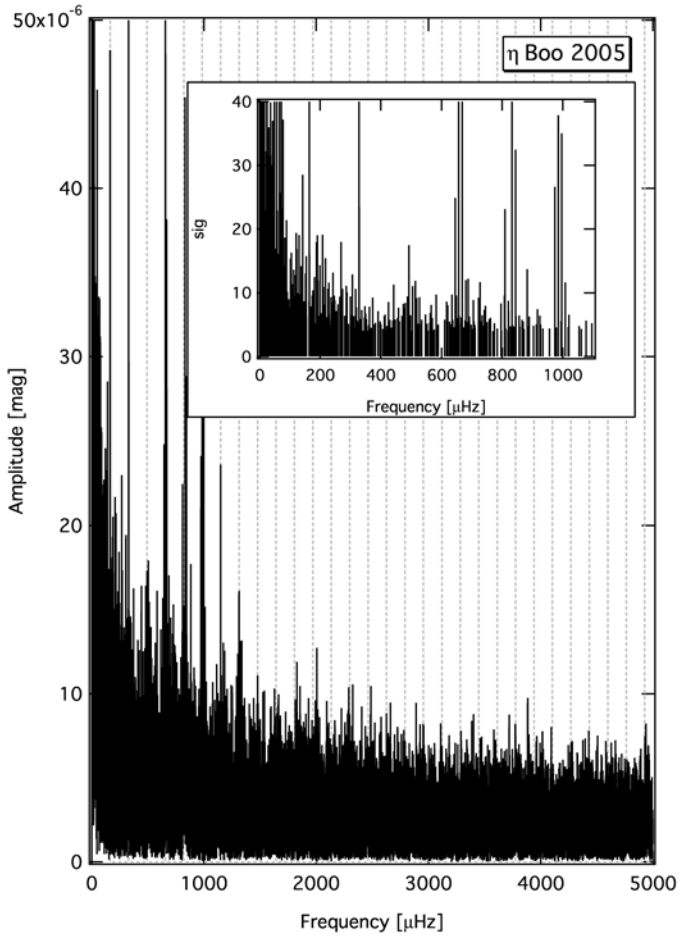


Figure 8: Same as Fig. 4. but for η Boo data.

of about 9 ppm, and those in Fig. 7 ($\text{sig} \geq 5.6$) have amplitudes ≥ 11 ppm. The frequencies plotted in Fig. 7 are different from those discussed in Guenther et al. (2005), because of the more rigorous and conservative approach adopted in this paper.

We also compared the observed echelle diagram with models from Guenther et al. (2005), as we did for Procyon above. The η Boo models are constrained by its luminosity and effective temperature (see Table 2), and the derived key

model parameters are shown in Table 3. Figure 7 also compares the averaged p -mode frequencies of the best-fitted models and the frequencies of the peaks in the 2004 and 2005 η Boo data sets with spectral significance ≥ 5.6 . η Boo has a more evolved core; hence, the nonradial p -modes are subject to mode bumping. As a consequence, the $l = 1, 2$ and 3 p -mode sequences do not fall along easily identifiable vertical sequences. Additionally, as noted in Guenther et al. (2005), the nonradial p -mode frequencies that are bumped are very sensitive to the age, mass, and composition of the model. Both effects in combination make model comparisons difficult. The radial p -modes identified in Guenther et al. (2005) lie outside of the indicated error bars, consistent with the fact that the best model fit to these modes was also just outside the 1σ observational uncertainty error box.

Constraints on mode lifetimes?

Since we do not see a clear radial ($l = 0$) sequence in any of our echelle diagrams for Procyon or η Boo, what is the origin of the peaks that remain in the target signal spectral significance spectrum after the background peaks have been removed? It seems unlikely that the remaining peaks are due to stray light since our identification of stray light in the background time series (BTS) is very effective. If they are intrinsic to the star, why do the observations from two epochs a year apart for the same star show so few frequencies in common (while the background spectral significance spectra for the same star in the two epochs are nearly identical)? Could this be a consequence of p -modes in these stars having short lifetimes?

Because the convective envelopes are shallow in these stars, the superadiabatic limit is closer to the optically thin surface than in the Sun, and the p -modes are subject to stronger radiative damping. This shortens their lifetimes compared to solar p -modes. The short lifetimes cause the amplitudes of the modes to vary on similar time scales, which in turn leads to modulation effects in the Fourier transform spectrum. The modulation effects include both splitting and smearing of the peaks. We must add that short 2 day variations could also be a consequence of variations in the forcing function itself. Robinson et al. (2005) found in their 3D numerical simulations of convection that the superadiabatic layer, the layer that provides most of the force driving turbulent convective motions, itself oscillates into and out of the very thin surface convective envelope in Procyon.

In an attempt to see if the identified peaks are the consequence of modulated amplitudes, we applied a running window 6 days wide to the TTS (target time series) of each star, and then applied our analysis routine to each windowed data set. We show a portion of the resulting time-evolving spectral significance

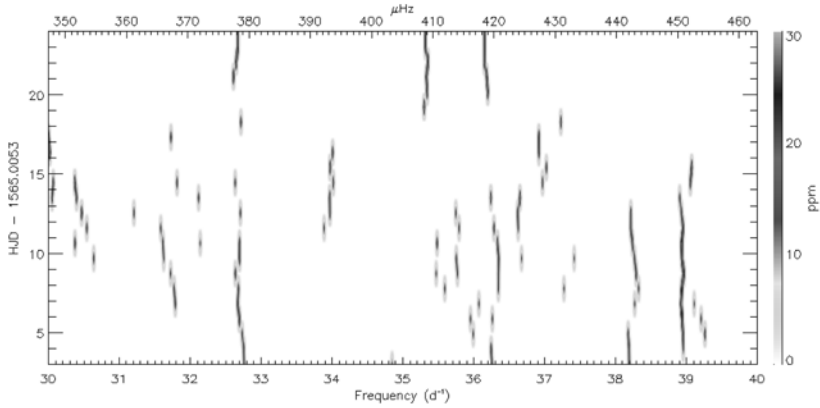


Figure 9: An intensity plot showing the changing amplitudes (and frequencies), over time, of peaks in the spectral significance spectrum of η Boo 2004 data. As individual peaks rise and fall in amplitude, they can shift in frequency and split into multiple peaks in the Fourier domain. Only a small portion of the spectral significance spectrum is shown.

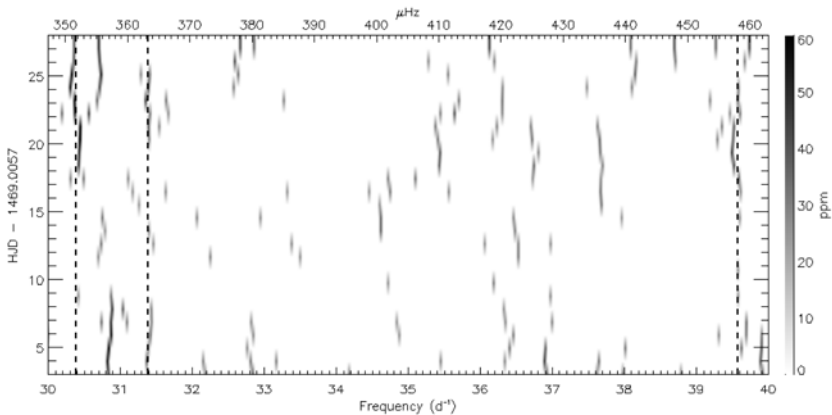


Figure 10: Same as Fig. 9 but for Procyon data.

spectrum for the 2004 η Boo data in Figure 9. As shown in Figure 10, similar results are seen for Procyon. These figures indicate that the peaks in the spectrum vary in amplitude over a timescale of about 2 days. The amplitude variation alone leads to perturbations in the frequency positions by approximately 0.5 cycle day^{-1} ($\sim 5 \mu\text{Hz}$).

If the peaks are p -modes and the modulation is intrinsic, then one has to dramatically expand the duration of the observation to give the damped and re-excited modes a chance to form well-defined Lorentzian profiles in the Fourier domain. If the length of observations is comparable to a modes lifetime (or only a few times longer) then the modes peak can fall over a relatively wide range of frequencies around the modes true frequency.

Conclusions

Analysis of the 2005 MOST photometry of Procyon and reanalysis of the 2004 data for that star reinforce the null p -mode detection reported by Matthews et al. (2004). The same type of analysis for the 2004 and 2005 MOST photometry of η Boo confirms the excess of power in the frequency range expected for p -modes but there is little agreement between identified frequencies in the two epochs. Our analysis suggests that the p -mode lifetimes in η Boo may be as short as about 2 days, which could account for the epoch-to-epoch differences. The groundbased spectroscopic campaigns on η Boo carried out by Kjeldsen et al. (2003) and Carrier et al. (2005) also do not identify the same frequencies in that star from epoch to epoch, which is also consistent with short mode lifetimes.

We have applied a more rigorous and conservative approach to stray light reduction than those used originally for the Procyon 2004 data (Matthews et al. 2004) and for the η Boo 2004 data (Guenther et al. 2005). In the former case, the high brightness of Procyon reduces the relative stray light effects, and our analysis affects only about 5-10% of the frequency range relevant for p -mode detection. In the case of the fainter η Boo, the new more aggressive treatment of stray light modulation gives a more robust identification of the intrinsic stellar frequencies. However, for this star, up to about 50% of the relevant frequency range may be affected.

We have produced p -mode model eigenspectra for Procyon and η Boo based on observed parameters of the two stars. However, the models cannot validate the frequency identifications in η Boo because the uncertainties in model parameters are too large. Even if we had evidence of p -modes in the photometry of Procyon, whose mass is well determined by its binary orbit, the uncertainties in the model eigenfrequencies would present a challenge to asteroseismic fitting. The possibility of short mode lifetimes makes the challenge even more severe.

The data presented here for Procyon and η Boo are available for download from the MOST Public Data Archive through the Science link at [http : //www.astro.ubc.ca/MOST](http://www.astro.ubc.ca/MOST).

Acknowledgments. The Natural Sciences and Engineering Research Council of Canada supports the research of D.B.G., J.M.M., A.F.J.M., S.M.R., G.A.H.W. A.F.J.M. is also supported by FQRNT (Québec), and R.K. is supported by the Canadian Space Agency. T.K, P.R. and W.W.W. are supported by the Austrian Research Promotion Agency (FFG), and the Austrian Science Fund (FWF P17580). The MOST Science Team would like to thank Sergey Marchenko (Western Kentucky University) for providing separate analysis stream results.

References

- Brown, T. M., Gilliland, R. L., Noyes, R. W., & Ramsey, L. W. 1991, ApJ 368, 599
- Carrier, F., Eggenberger, P., & Bouchy, F. 2005 A&A 434, 1085 (C05)
- Chaboyer, B., Demarque, P., & Guenther, D.B. 1999, ApJ 525, 41
- Christensen-Dalsgaard, J., & Frandsen, S. 1993, Solar Phys. 82, 469
- Eggenberger, P., Carrier, F., Bouchy, F., & Blecha, A. 2004, A&A 422, 247
- Girard, T. M., Wu, H., Lee, J. T., , et al. 2000, AJ 119, 2428
- Guenther, D. B., & Brown, K. 2004, ApJ 600, 419
- Guenther, D. B., Kallinger, T., Reegen, P., et al. 2005, ApJ 635, 547
- Houdek, G., Balmforth, N. J., Christensen-Dalsgaard, J., & Gough, D. O. 1999, AAP 351, 582
- Kjeldsen, H., & Bedding, T. R. 1995, A&A 293, 87
- Kjeldsen, H., Bedding, T. R., Baldry, I. K., et al. 2003, AJ 126, 1483
- Matthews, J. M., Kuschnig, R., Guenther, D. B., et al. 2004, Nature 430, 51
- Martic, M., Schmitt, J., Lebrun, J. C., et al. 1999, A&A 351, 993
- Reegen, P. 2005, Proceedings of the International Astronomical Union, Vol. 2004, No IAUS224, 791, (Cambridge: Cambridge University Press), also, <http://journals.cambridge.org/jidIAU>
- Reegen, P. 2006, Ph.D. dissertation, University of Vienna
- Reegen, P. 2007, A&A 467, 1353
- Robinson, F. J., Demarque, P., Guenther, D. B., et al. 2005, MNRAS 362, 1031
- Rucinski, S. M., Walker, G. A. H., Matthews, J. M., et al. 2004, PASP 116, 1093
- Walker, G. A. H., Matthews, J. M., Kuschnig, R., et al. 2003, PASP 115, 1023